

LA-UR-21-24446 (Accepted Manuscript)

Proton conductors for heavy-duty vehicle fuel cells

Kim, Yu Seung
Gittleman, Craig
Jia, Hongfei
De Castro, Emory
Chisholm, Calum

Provided by the author(s) and the Los Alamos National Laboratory (2021-11-08).

To be published in: Joule

DOI to publisher's version: 10.1016/j.joule.2021.05.016

Permalink to record: <http://permalink.lanl.gov/object/view?what=info:lanl-repo/lareport/LA-UR-21-24446>

Disclaimer:

Los Alamos National Laboratory, an affirmative action/equal opportunity employer, is operated by Triad National Security, LLC for the National Nuclear Security Administration of U.S. Department of Energy under contract 89233218CNA000001. By approving this article, the publisher recognizes that the U.S. Government retains nonexclusive, royalty-free license to publish or reproduce the published form of this contribution, or to allow others to do so, for U.S. Government purposes. Los Alamos National Laboratory requests that the publisher identify this article as work performed under the auspices of the U.S. Department of Energy. Los Alamos National Laboratory strongly supports academic freedom and a researcher's right to publish; as an institution, however, the Laboratory does not endorse the viewpoint of a publication or guarantee its technical correctness.

Perspective

Proton Conductors for Heavy-Duty Vehicle Fuel Cells

Craig S. Gittleman,¹ Hongfei Jia,² Emory De Castro,³ Calum Chisholm,⁴ and Yu Seung Kim^{5,6,*}

¹Global Fuel Cell Business, General Motors, Pontiac, Michigan 48340, USA

²Material Research Department, Toyota Research Institute of North America, Ann Arbor, Michigan 48105, USA

³Advent Technologies Inc. Cambridge, Massachusetts 02138-4946, USA.

⁴SAFCCell, Pasadena, California, 91106, USA

⁵MPA-11: Materials Synthesis and Integrated Devices, Los Alamos National Laboratory, Los Alamos, New Mexico 87545, USA

⁶Lead Contact

*Correspondence: yskim@lanl.gov

Fuel cells utilize the chemical energy of hydrogen, natural gas, or other hydrocarbon fuels to generate electricity. As fuel cells extend their territory to include heavy-duty vehicles, new demands for proton conductors, a critical component of fuel cells, have emerged. A near-term demand is ensuring the electrochemical and mechanical stability of proton exchange membranes to enable long life vehicle drive cycles. In the mid-term, the high conductivity and selectivity for proton vs. gas transport of proton conductors under hot and dry conditions are desirable. Ultimately, targeting high thermal stability and tolerance to water and impurities will save pay-load space of heavy-duty vehicles that may utilize high energy density liquid fuels. This article presents our perspective on these near, mid and long term targets for proton conductors of heavy-duty fuel cells.

Keywords: Fuel cell, Hydrogen, Proton exchange membrane, Conductivity, Gas transport, Heavy-duty vehicle, Liquid fuel, Performance, Durability, Heat management.

Context & Scale

Fuel cells are an attractive technology to power zero-emission vehicles. Compared to battery-powered vehicles, fuel cells offer fast fueling and adequate fuel storage for long-range applications. Heavy-duty fuel cell vehicles have strenuous requirements with the most urgent target being developing fuel cells with the durability to return capital costs over a longer lifetime. Fuel cell operation under hot and dry conditions may have benefits such as a reduction of radiator size and an increase in power density. Utilizing green liquid fuels can also save pay-load space and eliminate the need for an expansive hydrogen infrastructure. Proton conductors share the issues associated with heavy-duty fuel cell applications. Here, we present the progress and promising options for proton conductors in meeting near, mid, and long-term targets with respect to performance, durability, and technical readiness to stimulate research on proton conductors for heavy-duty fuel cells.

INTRODUCTION

The utilization and storage of hydrogen produced from renewable, nuclear, or fossil fuels with carbon capture can help decarbonize the U.S. and global economies and avoid the worst effects of climate change. In the mid-1970s, the United States Department of Energy (US DOE) touted the promise of hydrogen as a clean transportation fuel and consequently started polymer electrolyte membrane fuel cell (PEMFC) programs. The Energy Policy Act Title VIII on hydrogen in 2005 further promoted innovative hydrogen and fuel cell technologies. Recently, the US DOE Energy Efficiency Renewable Energy (EERE) Hydrogen and Fuel Cell Technologies Office (HFTO) initiated the H2@Scale concept for wide-scale hydrogen production and utilization¹. HFTO also announced the Million Mile Fuel Cell Truck Consortium (M2FCT) that supports early-stage R&D for widespread commercialization of heavy-duty vehicle (HDV) fuel cells. The 2025 target for M2FCT is to achieve 2.5 kW/g_{PGM} power (1.07 A/cm² current density) at 0.7 V after a 30,000 hour-equivalent of accelerated durability testing. Besides hydrogen fuel cells, interest in the utilization of clean liquid fuels is

growing because liquid fuels have a higher energy density and require significantly less infrastructure development costs. US DOE EERE HFTO and Advanced Research Projects Agency-Energy (ARPA-E) have supported fuel cell programs to implement various clean liquid-fuels.

Fuel cells convert hydrogen into a proton and electricity at the anode. The generated proton is transported through a proton exchange membrane (PEM) to react with oxygen and produce water at the cathode (**Figure 1A**). As fuel cells gain interest in HDV main powertrain applications, more stringent requirements for polymer electrolytes have been identified (**Figure 1B**). In the near-term, durability is the most urgent target for HDV fuel cell applications. According to US DOE’s multi-year research, development, and demonstration plan, 30,000 hour lifetime, approximately four times light-duty vehicles (LDV target: 8,000 hours²) is required for HDV applications³. In the mid-term, better heat and water management of fuel cells are the imperative targets. In current low-temperature proton exchange membrane fuel cells (LT-PEMFCs), the heat rejection requirement is met by operating the fuel cell at a high cell voltage, ca. 0.76 V at 80 °C, in which the generating power is < 0.4 W cm⁻². To achieve higher power, anhydrous proton conductors that can increase the operating temperature to > 100 °C is suggested. Additionally, PEMs with reduced gas crossover will be required to achieve DOE’s stringent 68% peak efficiency target². In the long-term, the utilization of clean liquid-fuel fuel cells is an attractive option due to the difficulties of transporting hydrogen over long distances and the low energy density of hydrogen. Since the reformation temperature of a broad range of hydrocarbon or carbon-free fuels takes place above 200 °C, a further increase in the operating temperature is desirable. Additionally, fuel cells require high tolerance to water and reformation by-products.

In this perspective article, we present the progress of next-generation proton conductors in meeting these requirements from the original equipment manufacturer’s view. Specifically, we focus on the current advancement of proton conductors in achieving high durability and better heat and water management by operating fuel cells at higher operating temperatures and utilizing high energy density liquid-fuels.

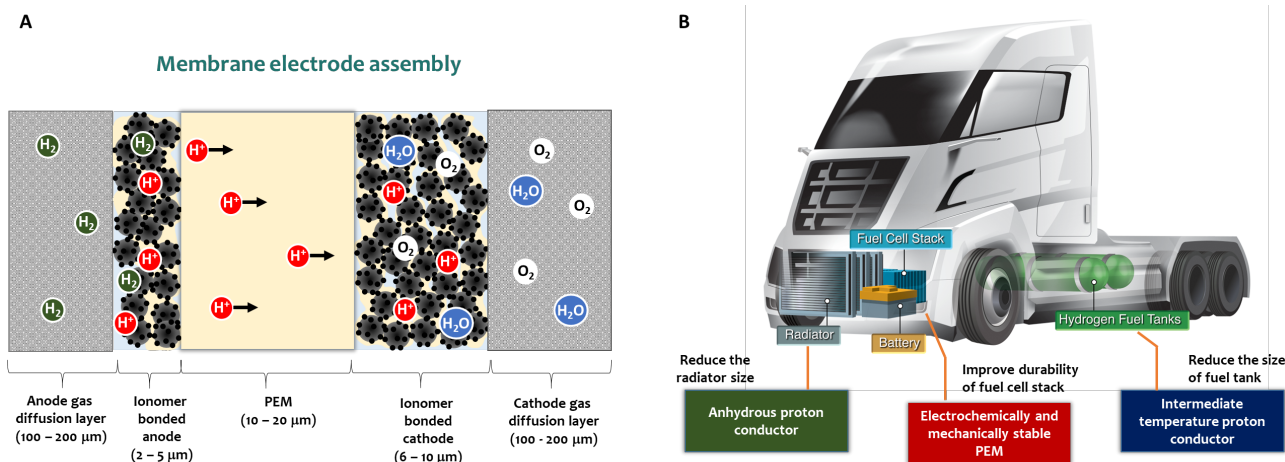


Figure 1. Proton conductors in fuel cells

(A) Schematic illustration of the cross-section of membrane electrode assembly (MEA) in a fuel cell and (B) benefits of advanced proton conductors for HDV fuel cell applications.

Proton Conductors for Durability – Near Term Challenge

Early fuel cell developments in 1995 reported 60,000 hours of durability during continuous fuel cell operation at 43 – 82 °C using a thick perfluorosulfonic acid (PFSA) PEM (Nafion 120, 250 μm-thick)⁴. However, the stability of PEMs became an issue as thinner membranes were employed for automotive fuel cells to increase power density. During the 2000s, the durability of fuel cells for bus was evaluated by Ballard Power Systems. Their P5 stacks (2002) with 50 μm-thick PFSA membranes lasted approximately 3,000 hours, while an HD6 module (2007) using a 25 μm-thick PFSA membrane ran for 6,842 hours.⁵ Since early-2010, various accelerated stress tests (ASTs) have been developed to evaluate the stability of PEMs within a shorter timeframe⁶⁻⁸. The ASTs were based on the fact that PEM degradation during

simultaneous chemical and mechanical stressors occurs much faster than individual stressor conditions^{6,9-10}. In a combined open-circuit voltage (OCV) and RH cycling AST protocol at 90 °C⁶, the PFSA membranes used for P5 and HD6 modules showed failure after ~100 and ~200 hours, respectively, when membrane cracking and local thinning were observed. A mechanically and chemically stabilized PFSA membrane (Nafion XL, 27.5 μm-thick)¹¹⁻¹² developed in 2010 failed after ~675 hours in this combined AST protocol. The thinning rate of the Nafion XL membrane was ~3 times lower than the PEM used for the Ballard HD6 module. The projected lifetime of a fuel cell using Nafion XL is ~20,000 hours, which is still lower than the DOE 2025 HDV target (30,000 hours). Thinner PEMs (10 – 15 μm) are currently used for LDV applications. A 12 μm-thick PEM used as an M2FCT benchmark passed the 8,000 hour LDV equivalent target in an AST¹³. Compared with PEMs for LDV applications, PEMs for HDV applications require better stability at higher operating temperatures because fuel cells run at a greater average power (**Figure 2A**). The average operating temperature of HDV fuel cells could be 5 – 15 °C higher, depending on the duty cycle, even if the peak operating temperature is maintained (**Figure 2B**).

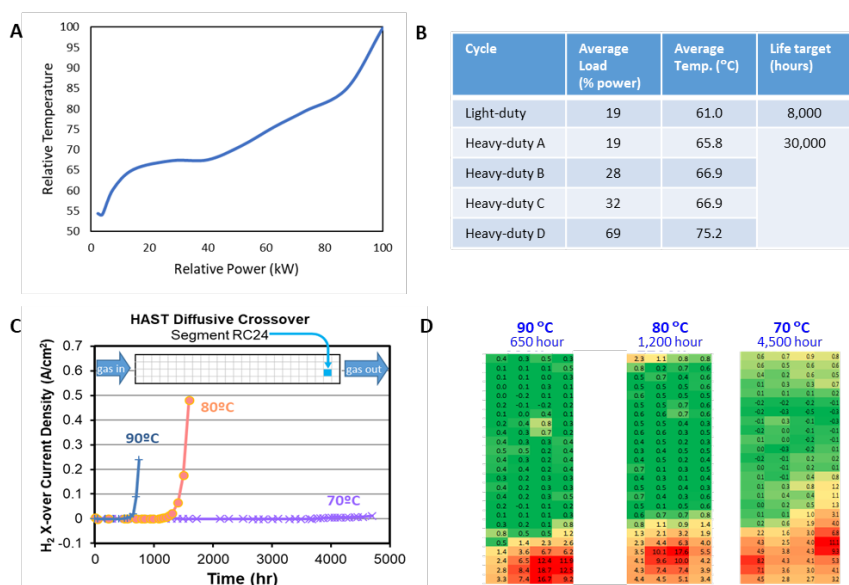


Figure 2. Impact of operating temperature on fuel cell durability

(A) Stack relevant coolant outlet temperature as a function of fuel cell load. (B) Average operating temperatures for a common fuel cell system operating under various LDV and HDV drive cycles. (C) Local H₂ diffusive crossover as a function of time for the combined AST tests at 70, 80 and 90 °C. (D) H₂ diffusive crossover maps towards the end of the combined AST tests at 70, 80 and 90 °C. Crossover values are in mA/cm². The data was reproduced from Ref.¹⁴

Operating temperature is one of the most significant factors that impact the durability of sulfonated PEM-based fuel cells¹⁴. **Figure 2C** shows the local hydrogen crossover current density change of PFSA-based fuel cells during GM’s combined AST as a function of temperature¹⁵. The cell operated at 70 °C shows initial signs of hydrogen crossover at 4,700 hours, while the cell operated at 80 °C failed to run after 1,600 hours. The lifetime of the cell at 90 °C is less than 750 hours. This combined stressor AST result is consistent with the durability tests of an 80 kW fuel cell system in which the cell life decreases by about half with each 10 °C temperature increase. The degradation process can be seen in the segmented hydrogen diffusive crossover maps measured towards the end of the test in **Figure 2D**. The *in-situ* diagnostic analyses indicated that the degradation progression of these cells is identical at the three temperatures. The membrane electrode assemblies (MEAs) tested at all three temperatures showed significant thinning of the PEMs towards the gas outlets. The post-mortem analyses indicated that PEM thinning occurs where the synergistic effect between mechanical and chemical stress is highest.

The chemical degradation of fuel cell membranes is mainly attributed to reactive free radical species that are generated *in-situ* through electrochemical pathways during fuel cell operation¹⁶. The most common and efficient way to improve the chemical stability of PFSA is to use radical scavengers. Ce, as either an ion or an oxide¹⁷⁻²⁰, and heteropolyacids (HPAs)²¹ are

potential radical scavengers that have proven to be effective. Small amounts of Ce incorporated into PFSA's effectively scavenges the reactive free radical species faster than they react with the polymer with minimal loss of membrane performance and mechanical durability¹⁰. HPAs, such as 11-silicotungstic acid, have been used to enhance proton conductivity under dry conditions, but the incorporation of HPA into PFSA's makes the PEM brittle²². Both Ce ions and HPA particles are mobile under fuel cell operating conditions, and PEM degradation can occur in more significant areas where the radical scavenger is depleted¹⁵. Therefore, concepts to immobilize the radical scavengers are being developed. One approach to immobilize Ce ions is to use cerium zirconium oxide (CeZr_xO_y) nanoparticles or nanofibers²³. An MEA using a CeZrO_4 -incorporated PFSA PEM showed a reduced fluoride release rate during the OCV test (Figure 3A) and negligible local Ce redistribution within the PEM after 85 hours at 1.0 A/cm², 80 °C and 100% RH (Figure 3B)¹³. For the immobilization of HPA, sulfonyl fluoride PFSA precursors with reactive anchor points were synthesized to tether HPA particles to the polymer through covalent bonds (Figure 3C)¹³. This approach also helps address the embrittlement observed in HPA-containing membranes. This is because when the HPA is tethered to a sulfonated ionomer rather than a non-functionalized polymer as in the previous studies²². There could be a much lower HPA concentration because they are not required for proton conductivity.

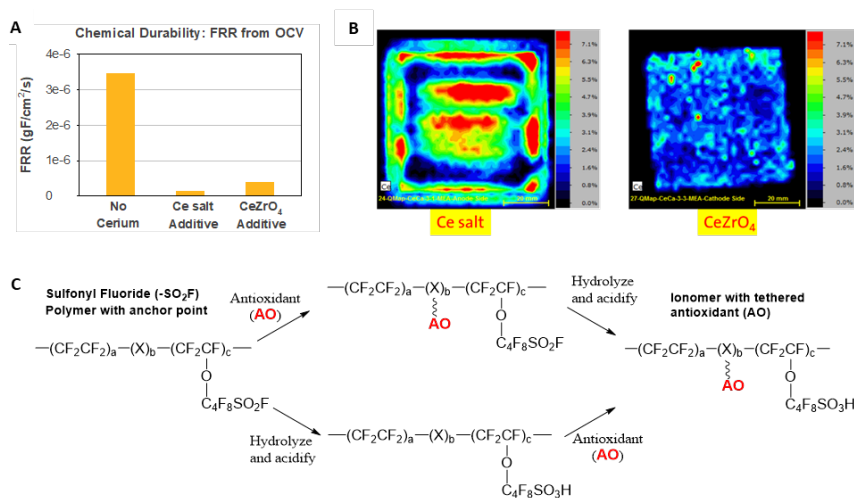


Figure 3. Approach to improve electrochemical stability of PEM.

(A) Fluoride release rate during 200 hour-OCV tests at 95 °C and 25% RH of PFSA membranes with and without Ce stabilizers; (b) Ce X-ray fluorescence map of Ce salt-stabilized PFSA membrane and $\text{Ce}_x\text{Zr}_y\text{O}_z$ nanofiber stabilized PFSA membrane after 85 hours at 1.0 A/cm², 80 °C and 100% RH in a 50 cm² serpentine flow field cell. (c) Reaction scheme of immobilizing HPA into a PFSA polymer using a sulfonyl fluoride polymer precursor. Reproduced from Ref.¹³ with permission.

Enhancing the mechanical stability of sulfonated PEMs is achieved mainly by incorporating structural reinforcements²⁴⁻²⁵ and utilizing high molecular weight ionomers²⁶. The most common and effective type of reinforcement or support layer is an expanded poly [tetrafluoroethylene] (ePTFE). The ePTFE's properties can be tailored to maximize durability by reducing in-plane membrane swelling while simultaneously minimizing proton transport losses.

Another approach to improve the stability of PEMs is to use sulfonated polyaromatics²⁷. Compared to the industrial standard PFSA PEMs, sulfonated polyaromatic PEMs have low hydrogen and oxygen permeability which improves not only fuel cell efficiency by reducing hydrogen crossover²⁸ but also the chemical stability of PEMs by decreasing hydrogen peroxide generation²⁹⁻³⁰. Furthermore, sulfonated aromatic PEMs have higher mechanical strength and modulus which makes it possible to cast thin film without reinforcement. However, the practical uses of sulfonated polyaromatic PEMs are limited by their strong dependence on RH for proton conductivity³¹, which requires a high level of humidification. Low conductivity at low RH can be improved by increasing the concentration of the sulfonic acid group. However, the incorporation of a high concentration of sulfonic acid groups in the polymers makes the PEMs brittle in a dry state and causes excessive swelling in a wet state. The brittleness of sulfonated polyaromatics in the dry state makes it difficult to handle while excessive swelling in the wet state increases mechanical stress, particularly at the edge of the MEA active area

where the hydration level of the PEM significantly changes³². Additionally, the high modulus of sulfonated aromatic PEMs, combined with their relatively high swelling, leads to exorbitant stress during humidity cycling which in turn leads to poor mechanical durability³³. As a result, most sulfonated polyaromatic PEMs cause premature MEA failures and do not survive during wet-dry cycling ASTs. More research efforts on improving the mechanical stability of sulfonated polyaromatic PEMs under wet-dry cycling conditions is necessary. Intrinsic susceptibility to radical-induced chain degradation of sulfonated polyaromatics also needs further study. This susceptibility cannot be addressed by the conventional stabilizers that work well with PFSA as the hydroxyl radical (HO•) reacts faster with the aromatic ring than it does with Ce³⁺³³.

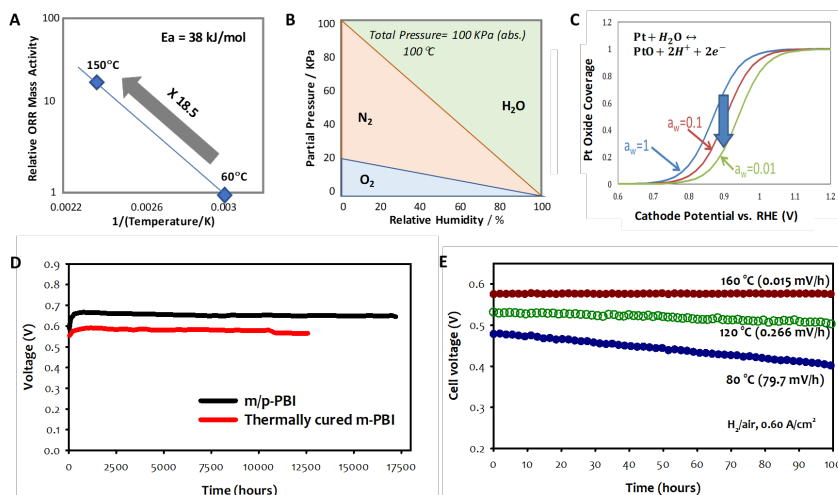


Figure 4. Impact of operating fuel cells under hot and dry conditions.

(A) catalytic activity of oxygen reduction reaction. (B) change of oxygen partial pressure as a function of RH. (C) Pt oxide coverage as a function of water activity³⁵. (D) PA-PBI HT-PEMFC durability³⁶. (E) Impact of operating temperature of durability of HT-PEMFC under anhydrous conditions. The H₂/air fuel cell performance was measured at a constant current density of 0.6 A/cm² under anhydrous conditions. 0% RH, cathode inlet, 0% RH.

Anhydrous Proton Conductors – Mid Term Challenge

The potential benefits of operating fuel cells under hot and dry conditions for vehicular applications include i) the use of low purity hydrogen or liquid fuels, ii) smaller radiator size *via* better thermal management, and iii) no need for a humidifier and a simplified flow channel design *via* anhydrous fuel cell operation³⁴. From the performance perspective, operating fuel cells under hot and dry conditions may enhance the catalytic activity, improve oxygen transfer *via* higher oxygen partial pressure by removing water in the MEA, and reduce Pt oxide formation in the absence of water (Figure 4A-C)³⁵. The operation of sulfonated PEM-based fuel cells under hot and dry conditions is challenging because sulfonic acid groups require water for the necessary proton conduction. Phosphoric acid-doped PEMs such as phosphoric acid-doped benzimidazoles (PA-PBIs) have reasonably high proton conductivity (~ 0.1 S cm⁻¹) and the PA-PBI-based fuel cells exhibited stable operation for a long time (e.g., > 17,000 hours at 160 °C³⁶, and > 10,000 hours at 180 °C³⁷) (Figure 4D)³⁸. The bottleneck of the automotive fuel cells employing PA-PBI PEMs is the cell stability at low operating temperatures (< 140 °C). Figure 4E shows the cell voltage change of PEMFCs using a PA-PBI PEM at three different operating temperatures (160, 120, and 80 °C). The fuel cell operating at 160 °C was stable with a low voltage decay rate (0.015 mV h⁻¹). However, as the operating temperature decreased to 120 and 80 °C, the voltage decay rate increased to 0.266 and 79.7 mV h⁻¹, respectively. The performance loss overtime at the low operating temperature is primarily related to phosphoric acid loss in the presence of water.

The phosphoric acid loss mechanism is related to the phosphoric acid equilibrium partition composition³⁹. Because the interaction energy of phosphoric acid-benzimidazole is lower than that of phosphoric acid-benzimidazole-water, the phosphoric acids in the polymer are replaced with water when exposed to the doped membrane to water. This phosphoric acid loss mechanism provides a pathway to improving phosphoric acid retention by introducing stronger ion-pair interactions (Figure 5A). Instead of using basic functionality, cation functionality can increase the equilibrium composition of phosphoric acid, and thus, water exchanges phosphoric acid in the polymer at a higher water vapor pressure. Lee et al. prepared an ion-pair membrane

that coordinated biphosphate anions and quaternary ammonium cations (PA-QAPOH)⁴⁰. The high phosphoric acid retention of the ion pair PEM was confirmed by temperature-cycling AST (80 to 160 °C) with a water partial vapor pressure of 9.7 kPa (**Figure 5B**). Note that the voltage of the PA-PBI MEA decreased from 0.78 to ~0 V within only 70 cycles. In contrast, the performance of the ion-pair MEA was stable during 500 thermal-cycles, maintaining the initial performance throughout the AST. The high acid retention of ion-pair coordinated polymers measured by the AST enables stable operation at 80 °C under high current generating conditions (~2 A cm⁻²).

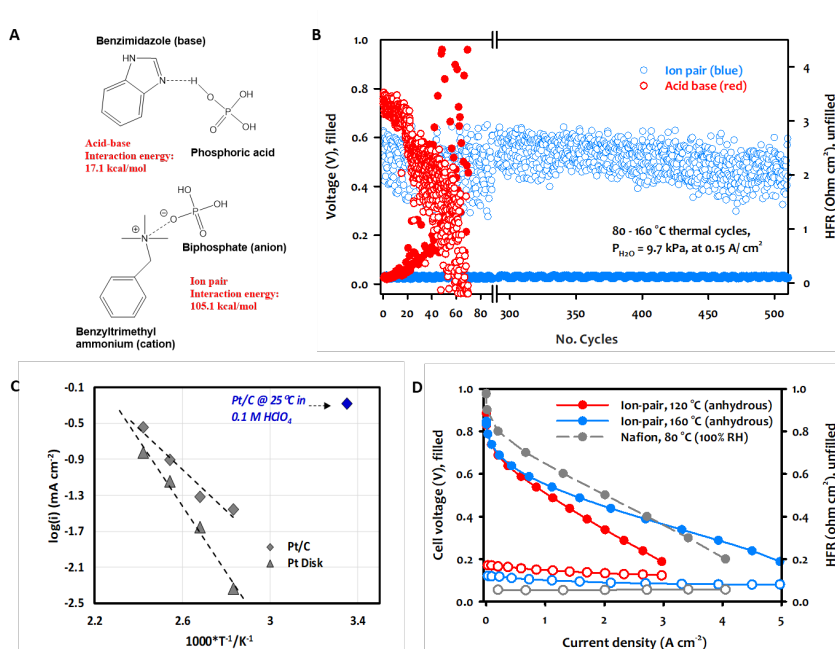


Figure 5. Approach to Prepare Anhydrous Proton Conductors.

(A) Interaction of PA-PBI acid-base and PA-QAPOH ion-pair polymer electrolytes. The interaction energy was calculated by DFT modeling³⁹. (B) Comparison of water tolerance between acid-base and ion-pair HT-PEMFC MEA. HFR and cell voltage change of the MEAs during thermal cycles of 80 – 160 °C under a constant water vapor pressure of 9.7 kPa. The cell was operated at a constant current density of 0.15 A/cm². Reproduced with permission⁴⁶. Copyright 2016, Springer Nature. (C) The ORR current density of Pt catalyst as a function of temperature. (D) H₂/O₂ fuel cell performance at 120 and 160 °C under anhydrous conditions. Ion-pair MEA, PEM: phosphoric acid doped quaternary ammonium polymer (PA-QAPOH) (PEM thickness: 40 μm), Anode catalyst: PtRu/C (0.5 mg_{Pt}/cm²), Cathode: Pt/C (0.6 mg_{Pt}/C). The fuel cell performance obtained the H₂/O₂ (500/500 sccm) under 147.1 kPa_{abs} backpressure without humidification. Nafion MEA, PEM: Nafion (PEM thickness: 25 μm), Anode catalyst Pt/C (0.6 mg_{Pt}/cm²), Cathode: Pt/C (0.6 mg_{Pt}/C). The fuel cell performance obtained the H₂/O₂ (500/500 sccm) under 285 kPa_{abs} backpressure with 100% RH. Reproduced with permission⁴⁵. Copyright 2020, Springer Nature.

One significant challenge of the ion pair PEM-based fuel cells is their performance. It is known that phosphoric acids can poison the catalysts with chemisorbed dihydrogen phosphate (H₂PO₄⁻) and hydrogen phosphate (HPO₄²⁻) ions⁴¹⁻⁴² as shown by a significantly lower oxygen reduction reaction (ORR) activity of Pt/C and Pt disk in phosphoric acid vs. perchloric acid (**Figure 5C**). Low oxygen permeability⁴³ and electrode flooding⁴⁴⁻⁴⁵ further lowers the electrode performance. Phosphonated polymers that have lower acid content may improve the performance for ion-pair MEAs⁴⁶. However, the performance of ion-pair MEAs in the kinetic region (> 0.7 V) is still substantially lower than a Nafion-based PEMFC (**Figure 5D**). Alloy catalysts that mediate the poisoning reaction, such as in typical phosphoric acid fuel cells, may improve the performance. Besides acid retention and fuel cell performance, start-up capability at low temperatures (-30 °C), development of high-temperature compatible non-functional materials (seals, gaskets, adhesives), and high-temperature corrosion and creep resistant materials require more attention to make the system suitable for HDV applications. However, many of these challenges, if not all, can be resolved by improving system design and control, including sealing strategies to eliminate the needs of polymer seals, carefully programmed startup and shutdown procedures to minimize the exposure to liquid water and stress from material thermal expansion/contraction and more efficient thermal management to reduce stack size. For example, operating HDVs at a rated power when over 100 °C enables the exploitation of latent heat systems (phase change of liquid coolant), which means many times greater heat

capacity than the sensible heat of any typical cooling fluid, which promotes small radiators and lower wind drag designs. The benefits of HT-PEMFCs can be further strengthened by choosing a range extender type of hybrid system, of which a large battery pack provides the main power for driving the motor, while the HT-PEMFC stack operates under the highly efficient steady-state condition to charge the batteries for extended driving distance. Such a hybrid platform not only helps overcome the inherent shortcoming of HT-PEMFC's slow startup but also takes advantage of the long lifetimes that have already been demonstrated under constant currents.

Proton Conductors for Liquid Fuels – Long Term Challenge

The major advantages of fuel cell-powered vehicles over battery-powered vehicles are high range and fast fuel refill time. Regardless, the low energy density of hydrogen fuel remains a technical barrier for HDV fuel cells. The volume of fuel and fuel tanks for diesel internal combustion engine with 50,000 lbs. load is 795 liters, whereas the volume of fuel and fuel tanks for the compressed hydrogen storage system of the fuel cell is 7,800 liters, approximately ten times greater⁴⁷. If the fuel is replaced by methanol, the volume of the fuel, fuel tanks and the reformer to store and convert the methanol to hydrogen through reforming is 2,460 liters (approximately 30% of the volume equivalent of compressed hydrogen). In addition to volume, working through these same metrics from a pure weight basis, a 50,000 lb. load would require 1,950 lbs. of diesel and tankage, or 12,920 lbs. of compressed hydrogen and tankage, or 7,560 lbs. of methanol, methanol tank, and a reformer capable of delivering less than 10 ppm CO. If a stack with HT PEM was employed, the weight and complexity of the reformer drops to the third stage, as typically 2 % CO is acceptable. Thus, liquid fuels as hydrogen carriers offer lower impact on load-carrying ability. Liquid fuels significantly reduce the hydrogen infrastructure problem as well. The global infrastructure cost for compressed hydrogen would be \$15,000 billion assuming a modest automotive penetration of 200 vehicles per 1,000 inhabitants, while the infrastructure cost for renewable liquid fuel only costs \$50 billion, 0.3% of the compressed hydrogen infrastructure cost due to the ability to use or modify existing infrastructure⁴⁸. The infrastructure cost for liquid fuel is even significantly lower than the battery infrastructure which would take \$5,000 billion.

A challenge for liquid fuel cells is the need for very fast reforming systems that can compete with hydrogen-based systems in overall specific and volumetric power density. Reformate hydrogen is problematic in LT-PEMFCs as the Pt electrocatalyst is very sensitive to CO poisoning. Pressure swing CO adsorption and gas-permeable membrane separation require very high pressures for separation and is therefore impractical for transportation applications⁴⁹. One simple solution to resolve the CO issue is to operate fuel cells at high temperatures (> 200 °C) under which electrode poisoning by CO can be minimized. **Figure 6A** shows the current density of a fuel cell at a constant voltage of 0.4 V at 240 °C in the presence of CO. The current density loss was 12% (1.14 to 1.0 A/cm²) with 25% CO, and the performance was completely recovered after pure hydrogen was reintroduced. Current reformer systems coupled with PEMFCs include water gas shift reactors to decrease the CO concentration to < 10 ppm.

Ideally, the reforming is done at the cell/stack level, that is, internal reforming, thus eliminating an external reformer. This also typically dictates a > 200 °C operational temperature. For example, **Figure 6B** shows a solid acid (e.g., CsH₂PO₄) fuel cell stack performance on various liquid and gaseous fuel reformates containing different CO concentrations. The MEAs used in the solid acid fuel cell stack incorporate a methanol steam reforming (MSR) catalyst in front of the hydrogen oxidation electrode. This allowed for direct MSR when running on methanol. The MSR layer also acts as a highly efficient CO water gas shift catalyst. As such, the externally reformed fuels, with a range of CO from 1 – 6%, have very similar performances with the net hydrogen concentrations (i.e., assuming full conversion of CO to hydrogen) being very similar, in the range of 41 – 60%.

Three different types of proton conductors have the potential to allow fuel cell operation at > 200 °C. The first are phosphoric acid-doped ion-pair PEMs. As explained in the previous section, these materials are composed of cation functionalized polymers doped with phosphoric acid. The advantage of these materials for fuel cells operating at 200 – 250 °C is their low ohmic resistance because acid-doped PEMs have high proton conductivity and can be produced as thin-film separators (~30 μm) (**Figure 6C**). Due to this resistance, the fuel cell power density is relatively high (910 mW/cm²) at 240 °C under H₂/air conditions (**Figure 6D**). There are two technical challenges to utilizing these materials for liquid fuel operations. First, phosphoric acid loss due to acid evaporation causes cell performance loss overtime when the fuel cell operates at > 220 °C. Second, phosphate poisoning by free acids lower OCV and kinetic performance. Phosphonic acids with low vapor pressure and minimal poisoning to fuel cell electrodes may need to be developed.

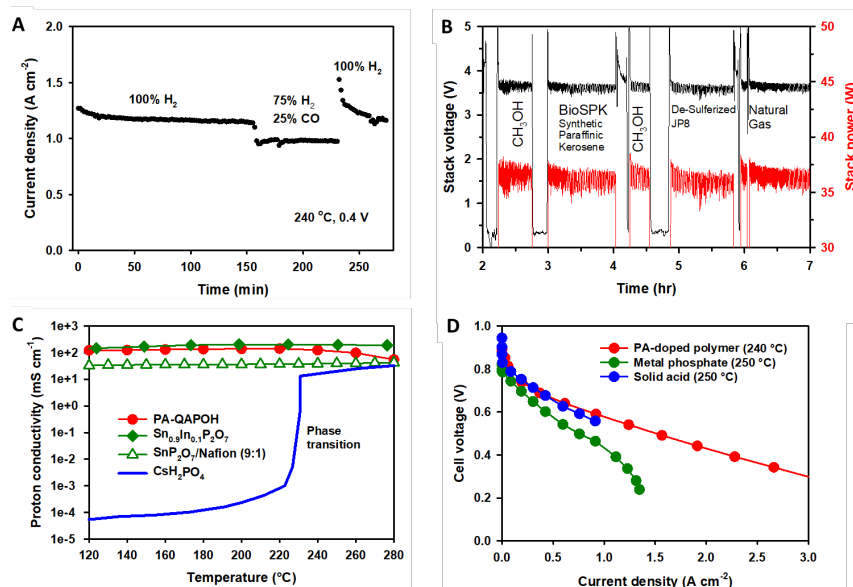


Figure 6. Performance of Intermediate Temperature Fuel Cells.

(A) Fuel cell performance test using simulated reformat conditions (75% H₂ – 25% CO) vs. O₂. Pt/C (0.6 mg_{Pt} cm⁻²) and PA-doped 90 wt% metal phosphate composite membrane (100 μm-thick) was used. (B) Fuel flexibility of fuel cell stacks operate at 250 °C. Stack: Solid acid fuel cells (5 cell stack, cell active area: ~ 100 cm², 10 A or 100 mA/cm²). Gas flows: Cathode: 50% utilization, air with 30% H₂O, Anode: 60 – 80% utilization, -reformat 30 – 50% H₂O. Gas compositions (dry): CH₃OH – 59% H₂, 1 % CO, JP8 (no S) – 38% H₂, 3% CO, BioSPK – 39% H₂, 5% CO, NG – 47% H₂, 6% CO. (C) Proton conductivity of PA-doped polymer (PA-QAPOH), metal phosphate-based (Sn_{0.9}In_{0.1}P₂O₇, and SnP₂O₇/Nafion composite) and solid acid (CsH₂PO₄) electrolytes in the temperature range of 120 – 280 °C. The data was taken from Ref.⁵¹ (D) H₂/air fuel cell performance of an MEA using PA-doped polymer, metal phosphate electrolyte and solid acid electrolyte. PEM: PA-QAPOH ion pair PEM (40 μm thick), Ionomer: phosphonated ionomer, Anode catalyst: Pt/C (0.6 mg_{Pt} cm⁻²), Cathode catalyst: Pt/C (0.6 mg_{Pt} cm⁻²). The performance was measured at 240 °C under backpressure of 147 kPa_{abs}. PEM: PA-doped SnP₂O₇/Nafion (9:1) composite (80 μm thick), ionomer: ion pair (PA-doped quaternary ammonium polystyrene), Anode catalyst: Pt/C (0.6 mg_{Pt} cm⁻²), Cathode catalyst: Pt/C (0.6 mg_{Pt} cm⁻²). The performance was measured at 250 °C under backpressure of 285 kPa_{abs}. MEA using the solid acid electrolyte. PEM: CsH₂PO₄ (50 μm thick), Anode catalyst: Pt/C (0.6 mg_{Pt} cm⁻²), Cathode catalyst: Pt-Pd alloy (1.3 mg_{Pt} cm⁻²). The performance was measured at 250 °C under backpressure of 141 kPa_{abs}, 30.4 kPa H₂O.

The second candidate material is a metal pyrophosphate (MP₂O₇, where M = Sn, Ti, Zr, W, Ce, Si, Ge). Indium doped tin pyrophosphate (Sn_{0.9}In_{0.1}P₂O₇) exhibited a proton conductivity of 195 mS cm⁻¹ at 250 °C⁵⁰. Recent studies on metal-doped and undoped tin pyrophosphates have shown that the crystalline phase itself possesses negligible protonic conductivity. However the presence of an excess amorphous polyphosphate phase is key for achieving high proton conductivity⁵¹. The advantage of these materials is stability and high conductivity over a wide temperature range (100 – 250 °C). However, making a thin-film separator is problematic due to the brittle nature of the metal phosphate particles. Therefore, the electrolyte separator was prepared from a polymer composite with 90 wt% SnP₂O₇ and 10 wt% Nafion (< 100 μm-thick membrane separator). Although the proton conductivity of the composite membrane was 40% of the SnP₂O₇ pellets (80 mS cm⁻¹ at 250 °C) (Figure 6C)⁵², the cell resistance can be reduced by the thin composite membrane. Reasonably high H₂/air performance (peak power density = 440 mW cm⁻² at 250 °C) was obtained (Figure 6D).

The third candidate material is the solid acid electrolyte. The general formula of the solid acid is M_xH_y(XO₄)_z (M = Cs, Rb, K, NH₄ and Ti, X = S, Se, P, As)⁵³. At low temperatures (< 200 °C), these materials are brittle, gas-permeable, water-soluble, and poor proton conductors. However, at high temperatures, these materials undergo a phase transition to possess plastic-like/gas impermeability, water-insolubility, and a reasonably high proton conductivity (ca. 20 mS cm⁻¹ at 250 °C). Figure 6C shows the proton conductivity of CsH₂PO₄ as a function of temperature. As noted, the phase transition occurs ~ 230 °C above which proton conductivity jumped to > 10 mS cm⁻¹⁵⁴. CsH₂PO₄ is thermodynamically stable as a solid at temperatures up to 300 °C, with proper hydration⁵⁵. This enables electrocatalyst particles to be deposited directly on the surface of sub-micron CsH₂PO₄ particles in the electrodes. Such an electrode, with Pt-Pd alloy nanoparticle resting on CsH₂PO₄ electrolyte particles used as a cathode for ORR exhibits viable performance (Figure 6D)⁵⁶⁻⁵⁷. Combined with the high impurity tolerances of the anode Pt/C catalyst and the ability to incorporate internal chemical catalysts for various reactions (e.g., steam reforming, CO water gas shift, ammonia decomposition, dehydrogenation), solid acid stacks can run on a wide variety of liquid fuels and reformat

streams with no or minimal reforming sub-system, greatly reducing system-level complexity and costs.

It is interesting to note that while “hotter is better” is the generally accepted mantra for high-temperature PEMs, there are additional challenges for running “hotter”. For example, while the possibility of directly oxidizing fuel at the anode has potential, this mode runs the risk of lower reaction yields compared to a more complete reforming and feeding reformat to the fuel cell. Therefore, highly active catalysts and electrode design of optimum mass transport architecture are needed. Furthermore, additional efficiency is gained by coupling the heat of the fuel cell with an external reformer. Another challenge of running too hot is finding the materials for MEA construction. Running over 260 °C eliminates most plastics and certainly, 300 °C restricts one of the most expensive gasket materials and questionable operation over 10,000 hours. Similarly, if one bases their system on unbound conducting elements (such as phosphoric acid absorbed in a matrix), 250 °C could be difficult. However, for simple fuels such as methanol, 220 °C is a reasonable match to what is needed for the complete thermal integration of a reformer. Bipolar plates have additional challenges when enlisted to operate at higher temperatures. But, in a low water/no water environment, bipolar plates could be freed from other material constraints associated with the liquid water environments of LT-PEMFCs, thus, bipolar plates can be stamped with simple metal components. Polymer seal materials with sufficient lifetimes (i.e., > 5,000 hours) at > 200 °C become limited and typically expensive. Also, for ORR, typical carbon-supported Pt group metal (PGM) catalysts, which have allowed for low PGM loadings with high catalytic activity, are not sufficiently robust to withstand accelerated fast carbon corrosion. As such, all > 200 °C liquid-fuel fuel cells will need to search for corrosion-resistant cathode catalysts to enable lifetimes of > 5,000 hours at low PGM loadings.

Outlook

Table 1 summarizes the performance and durability of fuel cells employing current proton conductors. More advanced proton conductors may enable resolution of technical challenges of fuel cells for heavy-duty applications. Development of thin and stable PEMs for LT-PEMFCs by immobilizing radical scavengers and mechanical reinforcement will enable fuel cell operation at high efficiency and with a longer lifetime. We expect < 20 μm thick electrochemically and mechanically stable PEMs will be developed in the next five years. The development of proton conductors having high conductivity under hot and dry conditions has shown notable progress over the last five years. Ion-pair PEMs have improved acid retention compared to conventional PA-PBI PEMs. Research towards increasing cell efficiency, improving start-stop durability, and developing other thermally-stable MEA components are encouraged. Prototype fuel cells that operate > 200 °C are attractive as future fuel cell technologies enable the use of liquid fuels through a direct *in situ* reformat process. Several proton conductors that have high proton conductivity have been developed. Thermal stability of stack and MEA components and cell durability remains a challenge to realize such fuel cells for automotive application.

Table 1. Fuel cell performance and durability employing current proton conductors

Approach		LT-PEM ¹³		HT-PEM						Intermediate Temperature			
				PA-PBI ^{36,58}		Ion-pair ⁴⁶				Metal P ₂ O ₇ ⁵³		Solid acid	
Temperature range (°C)		65 - 95		140 - 200		80 - 240				200 - 240		220 - 260	
Water vapor pressure (kPa)		4 - 100		0 - 10		0 - 20				Not available		0 - 40	
Lifetime (hours)		20,000 ^a (80 °C)		>17,000 ^b (160 °C)		> 550 ^c (160 °C)		Not available		900 ^d (220 °C)		> 8,000 ^e (250 °C)	
Power density (mW/cm ²)	at 0.7 V	840		120		80		230		120		340	
	Rated	380		450		480		910		430		440	
	Peak	1,400		450		550		at 240 °C		at 240 °C		at 250 °C	

^a Projected from AST equivalent.

^b Demonstrated at a constant current density of 0.2 A cm⁻² with 5 μV h⁻¹ voltage decay rate.

^c Demonstrated at a constant current density of 0.6 A cm⁻² with 0.35 μV h⁻¹ voltage decay rate.

^d Demonstrated at a constant voltage of 0.5 V.

^e Projected at a constant current density of 0.2 A cm⁻² with 20% voltage degradation.

AUTHOR CONTRIBUTIONS

Y.S.K proposed the idea. All authors wrote the manuscript.

ACKNOWLEDGMENTS

This work was supported by the US Department of Energy, Energy Efficiency and Renewable Energy, Hydrogen and Fuel Cell Technologies Office (HFTO) and Advanced Research Project Agency-Energy (ARPA-E). Los Alamos National Laboratory is operated by Triad National Security, LLC under U. S. Department of Energy Contract Number 89233218CNA000001.

REFERENCES AND NOTES

1. H2@Scale. (2020). U.S. DOE, Office of Energy Efficiency and Renewable Energy, Fuel Cell Technologies Office. <https://energy.gov/eere/fuelcells/h2scale>.
2. Fuel Cell Technologies Office Multi-Year Research, Development, and Demonstration Plan. 3.4 Fuel Cells (2017). U.S. DOE, U. S. Office of Energy Efficiency and Renewable Energy, https://www.energy.gov/sites/prod/files/2017/05/f34/fcto_myrd_d_fuel_cells.pdf.
3. Adams, J., (2020). DOE H₂ Heavy Duty Truck Targets. In *Compressed Gas Storage for Medium and Heavy Duty Transportation Workshop*, University of Dayton Research Institute, Dayton, OH 45469, <https://www.energy.gov/sites/prod/files/2020/02/f71/fcto-compressed-gas-storage-workshop-2020-adams.pdf>.
4. Steck, A. (1995). in *Proceeding 1st International Symposium. New Materials for Fuel Cell systems*. Savagodo, O.; Roberge, P. R.; Veziroglu, T. N., eds. p74.
5. Mukundan, R., James, G., Davey, J., Langlois, D., Torrace, D., Yoon, W., Weber, A. Z., and Borup, R. L. (2011). Accelerated testing validation. *ECS Trans.* *41*, 613-619.
6. Mukundan, R., Baker, A. M., Kusoglu, A., Beattie, P., Knights, S., Weber, A. Z., and Borup, R. L. (2018). Membrane accelerated stress test development for polymer electrolyte fuel cell durability validated using field and drive cycle testing. *J. Electrochem. Soc.* *165*, F3085-F3093.
7. Lim, C., Ghassemzadeh, L., Van Hove, F., Lauritzen, M., Kolodziej, J., Wang, G. G., Holdcroft, S., and Kjeang, E. (2014). Membrane degradation during combined chemical and mechanical accelerated stress testing of polymer electrolyte fuel cells. *J. Power Sources* *257*, 102-110.
8. Lai, Y. H., and Fly, G. W. (2015). In-situ diagnostics and degradation mapping of a mixed-mode accelerated stress test for proton exchange membranes. *J. Power. Sources* *274*, 1162-1172.
9. Kusoglu, A., Santare, M. H., Karlsson, A. M., Cleghorn, S., and Johnson, W. B. (2010). Numerical investigation of mechanical durability in polymer electrolyte membrane fuel cells. *J. Electrochem. Soc.* *157*, B705-B713.
10. Gittleman, C. S., Coms, F. D., and Lai, Y.-H. (2012). Membrane Durability: Physical and Chemical Degradation. In *Modern Topics in Polymer Electrolyte Fuel Cell Degradation* Mench, M., Kumbur, E. C., and Veziroglu, T. N., eds. (Academic Press).
11. Prabhakaran, V., Arges, C. G., and Ramani, V. (2011). Investigation of polymer electrolyte membrane chemical degradation and degradation mitigation using in situ fluorescence spectroscopy. *PNAS* *109*, 1029-1034.
12. Shi, S., Weber, A. Z., and Kusoglu, A. (2016). Structure/property relationship of Nafion XL composite membranes. *J. Membr. Sci.* *516*, 123-134.
13. Ramaswamy, N. (2020). Durable fuel cell MEA through immobilization of catalyst particle and membrane chemical stabilizer. In *US DOE Hydrogen and Fuel Cells Program: 2020 Annual Merit Review and Peer Evaluation Report*, https://www.hydrogen.energy.gov/pdfs/review20/fc323_ramaswamy_2020_p.pdf.
14. Healy, J., Hayden, C., Xie, T., Olson, K., Waldo, R., Brundage, A., Gasteiger, H., and Abbott, J. (2005). Aspects of the chemical degradation of PFSA ionomers used in PEM fuel cells. *Fuel Cells* *5*, 302-308.
15. Lai, Y.-H., Rahmoeller, K. M., Hurst, J. H., Kukreja, R. S., Atwan, M., Maslyn, A. J., and Gittleman, C. S. (2018). Accelerated stress testing of fuel cell membranes subjected to combined mechanical/chemical stressors and cerium migration. *J. Electrochem. Soc.* *165*, F3100-F3103.
16. Coms, F. D. (2008). The chemistry of fuel cell membrane chemical degradation. *ECS Trans.* *16*, 235-255.
17. Parabhakaran, V., Arges, C. G., and Ramani, V. (2012) Investigation of polymer electrolyte membrane chemical degradation and degradation mitigation using in situ fluorescence spectroscopy. *PNAS* *109*, 1029-1034.
18. Endoh, E. (2008). Development of highly durable PFSA membrane and MEA for PEMFC under high temperature and low humidity conditions. *ECS Trans.* *16*, 1229-1236.
19. Coms, F. D., Liu, H., and Owejan, J. E. (2008) Mitigation of perfluorosulfonic acid membrane chemical degradation using cerium and manganese ions. *ECS Trans.* *16*, 1735-1747.
20. Breitwieser, M., Klose, C., Hartmann, A., Buchler, A., Klingele, M., Vierrath, S., Zengerle, R., and Thiele, S. (2017). Cerium oxide decorated polymer nanofibers as effective membrane reinforcement for durable, high-performance fuel cells. *Adv. Energ. Mater.* *7*, 1602100.
21. Motz, A. R., Kuo, M.-C., Horan, J. L., Yadav, R., Seifert, S., Pandey, T. P., Galio, S., Yang, Y., Dale, N. V., Hamrock, S. J., and Herring, A. M. (2018). Heteropolyacid functionalized fluoropolymer with outstanding chemical durability and performance for vehicular fuel cells. *Energ. Environ. Sci.* *11*, 1499.
22. Herring, A. M., and Frey, M. (2012). Novel Approaches to Immobilized Heteropoly Acid (HPA) Systems for High Temperature, Low Relative Humidity Polymer-Type Membranes. In *US DOE Hydrogen and Fuel Cells Program: 2011 Annual Merit Review and Peer Evaluation Report*, https://www.hydrogen.energy.gov/pdfs/progress10/v_d_7_herring.pdf.
23. Baker, A. M., Williams, S. T. D., Mukundan, R., Spornjak, D., Advani, S. G., Prasad, A. K., and Borup, R. L. (2017). Zr-doped ceria additives for enhanced PEM fuel cell durability and radical scavenger stability. *J. Mater. Chem.* *5*, 15073-15079.
24. Cleghorn, S., Kolde, J., and Liu, W. (2003). Catalyst coated composite membranes. In *Handbook of Fuel Cells Volume 3: Fundamentals, Technology and Applications*, John Wiley & Sons, (New York) Vol. 3, pp 566-575.
25. Liu, F. Q., Yi, B. L., Xing, D. M., Yu, J. R., and Zhang, H. M. (2003). Nafion/PTFE composite membranes for fuel cell applications. *J. Membr. Sci.* *212*, 213-223.
26. Li, Y., Jiang, R., and Gittleman, C. S. (2020). Effects of melt flow index and equivalent weight on the dimensional stability and mechanical behavior of perfluorosulfonic acid ionomer membranes. *J. Power Sources* *478*, 228734.
27. Hickner, M. A., Ghassemi, H. Kim, Y. S. Einsla, B. R. and McGrath, J. E. (2004). Alternative polymer systems for proton exchange membranes (PEMs). *Chem. Rev.* *104*, 4587-4612.

28. Kim, J.-D., Ohira, A., and Nakao, H. (2020). Chemically crosslinked sulfonated polyphenylsulfone (CSPPSU) membranes for PEM fuel cells. *Membranes* *10*, 31.
29. Sethuraman, V. A., Weidner, J. W., Haug, A. T., and Protsailo, L. V. (2008). Durability of perfluorosulfonic acid and hydrocarbon membranes: Effect of humidity and temperature. *J. Electrochem. Soc.* *155*, B119-B124.
30. Miyake, J., Taki, R., Mochizuki, T., Shimizu, R., Akiyama, R., Uchida, M., and Miyatake, K. (2017). Design of flexible polyphenylene proton-conducting membrane for next-generation fuel cells. *Sci. Adv.* *3*, ea00476.
31. Einsla, M., Kim, Y. S., Hawley, M., Lee, H.-S., McGrath, J. E., Liu, B., Guiver, M. D., and Pivovar, B. S. (2008). Toward improved conductivity of sulfonated aromatic proton exchange membranes at low relative humidity. *Chem. Mater.* *20*, 5636-5642.
32. Ishikawa, H., Teramoto, T., Ueyama, Y., Sugawara, Y., Sakiyama, Y., Kusakabe, M., Miyatake, K., and Uchida, M. (2016). Use of a sub-gasket and soft gas diffusion layer to mitigate mechanical degradation of a hydrocarbon membrane for polymer electrolyte fuel cells in wet-dry cycling. *J. Power Sources* *325*, 35-41.
33. Gubler, L., Nausser, T., Coms, F. D.; Lai, Y.-H.; Gittleman, C. S. (2018). Perspective - prospects for durable hydrocarbon-based fuel cell membranes. *J. Electrochem. Soc.* *165*, F3100-F3103.
34. Greszler, T. (2006). Membrane Performance and Durability Overview for Automotive Fuel Cell Applications. In *DOE High Temperature Membrane Working Group*, https://www1.eere.energy.gov/hydrogenandfuelcells/pdfs/htmwg_greszler.pdf.
35. Suzuki, T. (2019). Towards future fuel cell vehicles: Challenge for 2040. In *PEFC&E19*, Atlanta, GA, pp 101B-1488.
36. Pingitore, A. T., Huang, F., Qian, G., and Benicewicz, B. C. (2019). Durable high polymer content m/p-polybenimidazole membranes for extended lifetime electrochemical devices. *ACS Appl. Energ. Mater.* *2*, 1720-1726.
37. Kannan, A., Aili, D., Cleemann, L. N., Li, Q. F., and Jensen, J. O., (2019). Three-layered electrolyte membranes with acid reservoir for prolonged lifetime of high-temperature polymer electrolyte membrane fuel cells. *Inter. J. Hydrog. Energy* *45*, 1008-1017.
38. Søndergaard, T., Cleemann, L. N., Zhong, L., Becker, H., Steenberg, T., Hjuler, H. A., Seerup, L., Li, Q., and Jensen, J. O. (2018). Catalyst degradation under potential cycling as an accelerated stress test for PBI-based high-temperature PEM fuel cells - Effect of humidification. *Electrocatalysis* *9*, 02-313.
39. Lee, A. S., Choe, Y. K., Matanovic, I., and Kim, Y. S. (2019). The energetics of phosphoric acid interactions reveals a new acid loss mechanism. *J. Mater. Chem.* *7*, 9867-9876.
40. Lee, K. S., Spendlow, J. S., Choe, Y. K., Fujimoto, C., and Kim, Y. S. (2016). An Operationally Flexible Fuel Cell Based on Quaternary Ammonium-Biphosphate Ion Pairs. *Nat. Energy* *1*, 16120.
41. He, Q. G., Yang, X. F., Chen, W., Mukerjee, S., Koel, B., and Chen, S. W. (2010). Influence of phosphate anion adsorption on the kinetics of oxygen electroreduction on low index Pt(hkl) single crystals. *Phys. Chem. Chem. Phys.* *12*, 12544-12555.
42. Li, Q., Wu, G., Cullen, D. A., More, K. L., Mack, N. H., Chung, H. T., and Zelenay, P. (2014). Phosphate-tolerant oxygen reduction catalysts. *ACS Catalysis* *4*, 3193-3200.
43. Gan, F., and Chin, D. T. (1993). Determination of diffusivity and solubility of oxygen in phosphoric-acid using a transit-time on a rotating ring-disc electrode. *J. Appl. Electrochem.* *23*, 452-455.
44. Eberhardt, S. H., Toulec, M., Marone, F., Stampanoni, M., Buchi, F. N., and Schmidt, T. J. (2015). Dynamic operation of HT-PEFC: in-operando imaging of phosphoric acid profiles and (re)distribution. *J. Electrochem. Soc.* *162*, F310-F316.
45. Kazdal, T., Lang, S., Kühn, F., and Hampe, M. J. (2004). Modeling of the vapour-liquid equilibrium of water and the in situ concentration of H₃PO₄ in a high temperature proton exchange membrane fuel cell. *J. Power Sources* *249*, 446-456.
46. Atanasov, V., Lee, A. S., Park, E. J., Maurya, S., Baca, E. D., Fujimoto, C., Hibbs, M., and Kerres, J. (2020) Synergistically Integrated Phosphonated Poly(pentafluorostyrene)s for Fuel Cells. *Nat. Mater.* DOI: [10.1038/s41563-020-00841-z](https://doi.org/10.1038/s41563-020-00841-z).
47. Methanol Fuel Cells: Powering the Future, Tim Chan, Methanol Institute. (2020). *Element 1 Corp presentation*. <https://3xxngg2wmai7100rss2cgkmj-wpengine.netdna-ssl.com/wp-content/uploads/2020/04/Methanol-Fuel-Cell-Powering-the-Future-webinar-presentation.pdf>.
48. Shih, C. F., Zhang, T., Li, J., and Bai, C. (2018). Powering the future with liquid sunshine. *Joule* *2*, 1925-1949.
49. Amphlett, J. C., Creber, K. A. M., Davis, J. M., Mann, R. F., Peppley, B. A., and Stokes, D. M. (1994). Hydrogen-Production by Steam Reforming of Methanol for Polymer Electrolyte Fuel-Cells. *Int J Hydrogen Energy* *19*, 131-137.
50. Nagao, M., Kamiya, T., Heo, P., Tomita, A., Hibino, T., and Sano, M. (2006). Proton conduction in In₃-doped SnP₂O₇ at intermediate temperatures. *J. Electrochem. Soc.* *153*, A1604-A1609.
51. Kreller, C. R., Pham, H. H., Wilson, M. S., Mukundan, R., Henson, N., Sykora, M., Hartl, M., Daemen, L., and Garzon, F. H. (2017). Intragranular phase proton conduction in crystalline Sn_{1-x}In_xP₂O₇ (x=0 and 0.1). *J. Phys. Chem. C* *121*, 23896-23905.
52. Lee, K. S., Maurya, S., Kim, Y. S., Kreller, C. R., Wilson, M. S., Larsen, D., Elangovan, S. E., and Mukundan, R. (2018). Intermediate temperature fuel cells via an ion-pair coordinated polymer electrolyte. *Energy Environ. Sci.* *11*, 979-987.
53. Haile, S. M., Boysen, D. A., Chisholm, C. R. I., and Merle, R. B. (2001). Solid acids as fuel cell electrolytes. *Nature* *410*, 910-913.
54. Haile, S. M., Chisholm, C. R. I., Sasaki, K., Boysen, D. A., and Uda, T. (2007). Solid acid proton conductors; from laboratory curiosities to fuel cell electrolytes. *Fradaday Discuss.* *134*, 17-39.
55. Boysen, D. A., Uda, T., Chisholm, C. R. I., and Haile, S. M. (2004). High-performance solid acid fuel cells through humidity stabilization. *Science* *303*, 68-70.
56. Chisholm, C. R. I., Boysen, D. A., Papandrew, A. B., Zecevic, S., Cha, S., Sasaki, K., Varga, A., Giapis, K. P., and Haile, S. M. (2009). From laboratory breakthrough to technological realization: The development path for solid acid fuel cells. *Electrochem. Soc. Interface*, *Fall*, 35-41.
57. Papandrew, A. B., Chisholm, C. R. I., Zecevic, S. K., Veith, G. M., and Zawodzinski, T. A. (2013). Activity and evolution of vapor deposited Pt-Pd oxygen reduction catalysts for solid acid fuel cells. *J. Electro. Chem. Soc.* *160*, F175-F182.

58. De Castro, E. (2009). In *PBI-phosphoric acid based membrane electrode assemblies: status update*, PAFC Workshop, <https://www.energy.gov/eere/fuelcells/downloads/pbi-phosphoric-acid-based-membrane-electrode-assemblies-status-update>.